NANO LETTERS
Letter
pubs.acs.org/NanoLett

Conformation-Dependent Photostability among and within Single Conjugated Polymers

Heungman Park,[†] Dat Tien Hoang,[†] Keewook Paeng,[†,‡] Jaesung Yang,[†] and Laura J. Kaufman*,[†]

[†]Department of Chemistry, Columbia University, New York, New York 10027, United States
[‡]Department of Chemistry, Sungkyunkwan University, Suwon 440-746, Republic of Korea

Supporting Information

ABSTRACT: The relationship between photostability and conformation of 2-methoxy-5-(2′-ethylhexyloxy)-1,4-phenylenevinylene (MEH-PPV) conjugated polymers was studied via excitation polarization modulation depth (*M*) measurements. Upon partial photobleaching, *M* distributions of collapsed, highly ordered MEH-PPV molecules shifted toward lower values. Conversely, *M* distributions of MEH-PPV molecules with random coil conformations moved toward higher values after partial photobleaching. Monte Carlo simulations of randomly distributed dipole moments along polymer chains subjected to partial photobleaching revealed that a statistical effect leads to an increase in peak *M* value. Decreases in *M* values seen experimentally in the population of MEH-PPV molecules with high *M* values, however, are due to conformation-dependent photostability within single MEH-PPV polymers. We show that, while folded MEH-PPV molecules are relatively more photostable than extended MEH-PPV molecules in an ensemble, extended portions of particular molecules are more photostable than folded domains within single MEH-PPV molecules.

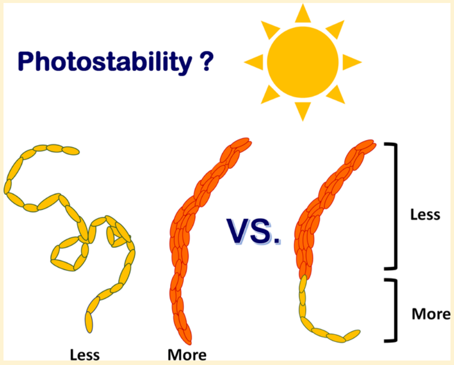

KEYWORDS: *Conjugated polymer, MEH-PPV, fluorescence, modulation depth, exciton migration, photobleaching*

Conjugated polymers are attractive for applications in electronics and optoelectronics due to their photophysical and material properties that present opportunities for the development of robust, low-cost, easily processable devices. While conjugated polymers have desirable properties for use in next-generation devices, the heterogeneous nature of polymer conformation and interactions presents complications. One particular difficulty is the fact that heterogeneities in chain conformation affect photophysical properties of the chain as well as interactions between chains. For example, the preference for an exciton to undergo across- (or inter-) chain vs along- (or intra-) chain migration depends on the degree of chain folding present.[1−6]

Information about single conjugated polymer morphology has commonly been extracted by characterizing single molecule absorption of polarized light. A chromophore maximally absorbs light whose polarization is parallel to its transition dipole and does not absorb when it is perpendicular. Since conjugated polymers are composed of many absorbing units, polarized light will selectively excite a subset of the absorbers according to their alignment with the polarization of the excitation light. Conjugated polymers with highly aligned absorbing chromophores will have an absorption cross-section and fluorescence intensity that varies significantly as a function of polarization angle of the excitation light. Conjugated polymers with absorbing chromophores oriented at random will display limited modulation in absorption and fluorescence as a function of excitation light polarization.

Such differences in orientation of absorbing chromophores have typically been characterized by measuring polarization modulation depth (*M*) as obtained via

$$I(\phi) = I_0[1 + M\cos\{2(\phi - \phi_0)\}] \tag{1}$$

with $I(\phi)$ fluorescence intensity as a function of ϕ, the angle of the excitation polarization. I_0 is average emission intensity and ϕ_0 is a reference polarization angle corresponding to the maximum intensity. M can be calculated equivalently from $M = (I_{\max} - I_{\min})/(I_{\max} + I_{\min})$, the ratio of modulation intensity amplitude to average intensity. This technique has been used, for example, to demonstrate trends in chain conformation as a function of intermolecular interactions between the polymer and host matrix.[7−16]

Despite the straightforward theoretical underpinnings and instrumentation required for polarization modulation depth measurements, reproducibility of such measurements is not assured. For a given type of conjugated polymer in a given host matrix, there have been differing reports of *M* distributions.[8,10] Such differences may emerge from differences in sample preparation or storage conditions and include possible aggregation, presence of chemical defects, and/or thermal or optical degradation of the conjugated polymers.[3,8,10,14,17−22]

Received: August 25, 2015
Revised: October 2, 2015
Published: October 6, 2015

ACS Publications © 2015 American Chemical Society

DOI: 10.1021/acs.nanolett.5b03409
Nano Lett. 2015, 15, 7604−7609

Details of data analysis, including feature identification and background determination and subtraction, can also affect reported M values.

One consistent finding is that the photophysical behavior of immobilized 2-methoxy-5-(2′-ethylhexyloxy)-1,4-phenylenevinylene (MEH-PPV) molecules depends on the dissolving solvent used before immobilization of these conjugated molecules into a host matrix.[1,3,5,15,16,23] Observations of absorption spectra, polarization modulation depth, intensity trajectories, and positions of the emitting chromophores all suggest that choice of solvent affects conjugated polymer conformation in a given host. In particular, measurement of polarization modulation depth of isolated single MEH-PPV polymers prepared from dissolution in chloroform before immobilization in poly(methyl methacrylate) showed lower M values on average than those molecules prepared from dissolution in toluene.[15,16] Such experimental observations support the view that, in a given host matrix, immobilized MEH-PPV molecules prepared from chloroform are present in a relatively open random coil conformation compared to those prepared from toluene, which are believed to be in highly ordered folded states. It has been suggested that MEH-PPV molecules in a random coil conformation will have many isolated absorbing and emitting units, leading to high fluorescence intensity, continuous fluorescence intensity decay with photobleaching, and low M values due to the large number of noninteracting chromophores along the backbone. Highly folded and ordered MEH-PPV molecules, on the other hand, are expected to display stepwise photobleaching trajectories, due to the efficient across-chain exciton migration to a small number of emitting chromophores, and high M values, due to alignment of those chromophores as would exist in ordered molecular conformations.[1,3,5,19,20]

In this study, we reproduce the finding that the M distribution differs for MEH-PPV molecules spin-coat from toluene and chloroform solutions and demonstrate that M distributions are sensitive to partial photobleaching. In particular, among MEH-PPV molecules prepared from initial dissolution in chloroform, we show that partial photobleaching consistently leads to modulation depth histograms that peak at higher values relative to those of unbleached molecules. Simulations reveal that a portion of the change in modulation depth distribution upon partial photobleaching can be accounted for by the statistics associated with the decreasing number of chromophores. However, that change cannot account for all observations in this study. Instead, we propose that statistical effects and conformation-dependent photobleaching both across and within single MEH-PPV molecules combine to produce the observed effects. The findings presented here suggest that MEH-PPV molecules existing in random coil conformations are less photostable than those in highly ordered arrangements; conversely, on a given MEH-PPV molecule, unfolded domains are relatively more photostable than folded ones.

MEH-PPV (M_w = 168 kDa, PDI = 2.1) was synthesized following a previous report.[24] MEH-PPV was diluted in ∼4 wt % polystyrene (M_W = 6.4 kDa, PDI = 1.05) with either toluene or chloroform as the solvent. Films of ∼200 nm thickness were prepared by spin-casting the solution onto native oxide covered silicon wafers. The concentration of MEH-PPV in the solution was $\sim 10^{-11}$ M resulting in average separation between molecules of greater than 1 μm. No sonication was used at any point in sample preparation to avoid possible scissioning.[17] Experiments were performed on a home-built wide-field epifluorescence microscope equipped with a vacuum cryostat. Excitation light at 532 nm from a continuous wave laser was employed to perform M measurements and partial photobleaching. Movie data was analyzed using procedures written in Python.[25,26] M values were obtained by fitting data to eq 1. Detailed experimental and analysis procedures are described in the SI.

Excitation modulation depth measurements were performed on MEH-PPV molecules immobilized in a polystyrene (PS) matrix following dissolution in chloroform or toluene. Median modulation depth for chains prepared from dissolution in toluene was higher than for those prepared from dissolution in chloroform (Figure S3), in accordance with previous results.[15,16] While this finding has been reported previously, quantitative differences between reports exist, and these differences may be due to sample preparation and storage conditions and/or differences in data analysis procedures. One potential source of variation between the findings is optical degradation of the conjugated polymers that can occur through exposure to light, including typical room light. Figure 1 shows normalized M distributions for populations of MEH-PPV polymers prepared from dissolution in chloroform after 8 and 22 h of exposure to a 23 W compact fluorescent lamp or while shielded from the lamp. Following exposure, the excitation modulation depth distribution was shifted to higher values.

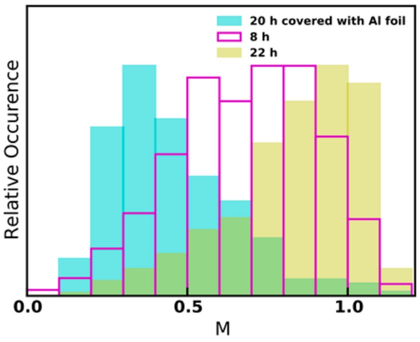

Figure 1. Normalized M distributions of MEH-PPV molecules in a PS matrix prepared from dissolution in chloroform exposed to a compact fluorescent light for 20 h with the samples covered with aluminum foil (227 features, median M = 0.42, median intensity = 1695 arbitrary units [a.u.]), 8 h without aluminum foil (240 features, median M = 0.70, median intensity = 1070 a.u.), and 22 h without aluminum foil (351 features, median M = 0.87, median intensity = 669 a.u.).

To investigate this behavior under more controlled conditions, measurements were repeated with a laser beam as described in the SI. The manner in which the experimental data was collected allowed investigation of not only average modulation depth for a set of molecules but also allowed following excitation modulation depth and fluorescence intensity of each interrogated MEH-PPV molecule before (M measurement), during (intensity measurement), and after (M measurement) moderate intensity light exposure. A set of measurements for a representative single molecule is described in the SI and shown in Figure S4. The increase in M and retention of the photobleaching behavior (continuous or stepwise) seen for this exemplary molecule was typical, as evidenced by the M values measured for the full set of molecules interrogated (Figure 2a,c). This shift is consistent with the shift in M distribution seen following exposure to a

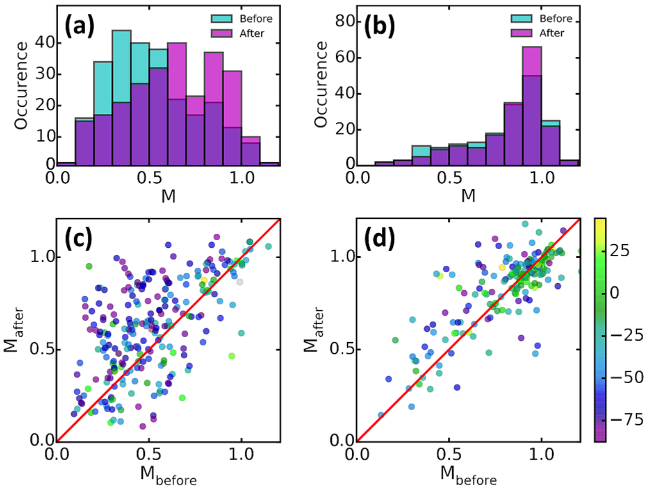

Figure 2. Histograms and scatter plots of M distributions before and after partial photobleaching of MEH-PPV molecules prepared from dissolution in (a, c) chloroform or (b, d) toluene. Figure S5 shows the scatter plots with error bars. Median M = 0.49 (before) and 0.63 (after) for chloroform and M = 0.87 (before) and 0.90 (after) for toluene. Color indicates relative intensity change during the photobleaching period. Median change in intensity in the molecules prepared from chloroform was −55.1% and in those from toluene was −24.1%.

fluorescent lamp (Figure 1). The trend toward increasing M upon partial photobleaching seen for MEH-PPV molecules prepared from chloroform was somewhat less obvious among molecules prepared from toluene (Figure 2b,d); however, a shift to higher M values upon partial photobleaching was also apparent, particularly in molecules that initially had low M values (Figure 2d).

During the partial photobleaching process that occurs between the two polarization modulation measurements, nearly all molecules experienced a decrease in overall fluorescence intensity, as expected. This decrease in intensity is driven by a decrease in number of chromophores, which itself may have an effect on M. To interrogate whether decrease in number of chromophores alone could explain the trend in modulation depth measured before and after partial photobleaching, 2D and 3D Monte Carlo simulations were performed.

In the simulations, transition dipoles representing those on a single polymer were randomly distributed, as in a freely jointed-chain (FJC). All transition dipoles were assumed to be within a diffraction-limited spot, and absorption and emission chromophores were conflated. Given these assumptions, a molecule with two transition dipoles on a plane will exhibit $M = 0$ if they are perpendicular to each other and $M = 1$ if they are parallel. The dependence of M on angle between the two transition dipoles is shown in Figure S6. For this case, as well as cases in which each simulated polymer has more than two transition dipoles, M was calculated from the incoherent sum of the square of the transition dipoles in each polymer. The expected M distributions for a population of molecules with $N = 1-1000$ transition dipoles are shown in Figure 3 for 2D and 3D FJC simulations. The peak shifts toward higher M values as the number of transition dipoles decreases. 3D simulations within the FJC model show similar results since the projection of each transition dipole onto a 2D plane follows the same statistics, with different amplitude depending on the out-of plane orientation of each transition dipole.

It has been shown that the number of monomers in a single conjugation unit in MEH-PPV is 5−20.[27−29] Thus, the 168 kDa MEH-PPV molecules used in these experiments may be expected to have 30−160 absorbing units. If the transition dipoles are randomly distributed, the measured M distribution would be expected to resemble the distributions of the FJC model simulated for between 10 and 100 transition dipoles. The M distributions of MEH-PPV molecules prepared from dissolution in chloroform as shown in Figure 1 and Figure 2a do bear resemblance to these distributions in breadth and peak position, with greater resemblance to the $N = 10$ than $N = 100$ simulated distribution. It has recently been pointed out that actual MEH-PPV molecular weight may be smaller than that reported by gel-permeation chromatography,[30] which may explain why the M distributions are most consistent with molecules with relatively few chromophores. Another factor may be that the wavelength of the excitation laser used in this study is near the edge of the MEH-PPV absorption, potentially limiting the number of absorbing chromophores.[3,19,31] The M distribution of MEH-PPV molecules prepared from toluene does not resemble any of the simulated distributions in Figure 3, consistent with the suggestion that these molecules are in highly ordered conformations that are not approximated by the random distribution of transition dipoles in the simulation.

In addition to capturing the general characteristics of the M distribution measured for MEH-PPV molecules dissolved in chloroform, the simulations presented above suggest that with a

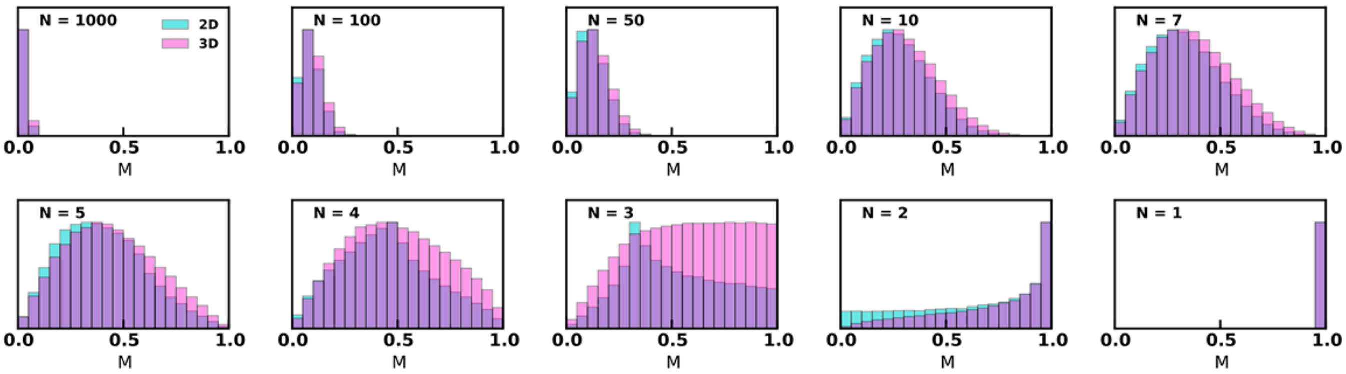

Figure 3. Normalized M distributions from Monte Carlo simulations within the freely jointed chain model as a function of number (N) of transition dipoles oriented at random in 2D (cyan) and 3D (magenta). At least 100 000 polymers were generated for each simulation to obtain smooth distributions.

decrease in number of chromophores, as occurs during partial photobleaching, the median M value would increase for purely statistical reasons. To fully capture the effects of partial photobleaching, however, requires including stochastic effects that may lead to greater decrease in number of chromophores on some molecules than on others. To model this, a partial photobleaching simulation was performed. An ensemble of polymers was generated with a fixed number of transition dipoles, and transition dipoles were removed at random as described in the SI. As a result, simulated polymers with a broad distribution of number of transition dipoles were present after this simulated bleaching. *M* distributions were calculated before and after simulated partial photobleaching. The 2D and 3D FJC simulations confirm that, within this model, a shift right and broadening of the *M* distribution is expected upon partial photobleaching (Figure 4, Figure S7).

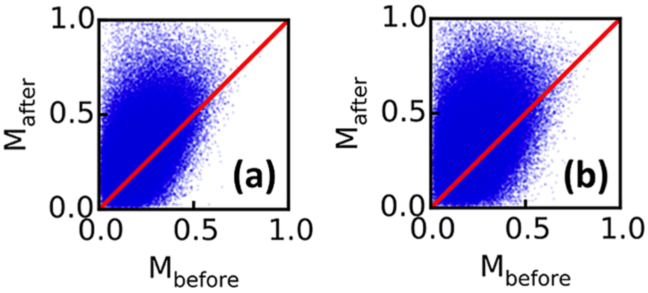

Figure 4. (a) 2D and (b) 3D FJC model photobleaching simulations. The initial number of transition dipoles is 15. Histograms and intensity change plots are shown in Figure S7. Median *M* = (a) 0.22 (before) and 0.32 (after), and (b) 0.24 (before) and 0.35 (after).

It is challenging to directly compare the shift seen upon partial photobleaching in these simulations to those measured in experiment because even though the initial simulated *M* distributions bear resemblance to those measured, they do peak at lower *M* values. Indeed, it is possible that in a distribution that initially peaks at higher values, the statistical effects seen upon partial photobleaching here would not be apparent. To assess this possibility, simulations of a more realistic polymer model were performed. Here, a freely rotating-chain (FRC) model that restricts angular change between transition dipoles was employed to incorporate the rigidity of the MEH-PPV polymer into the simulation.[32] Results of Monte Carlo simulations of *M* distributions within the 3D FRC model as a function of number of transition dipoles with chain-to-chain angle of either 45 or 30 degrees are shown in the SI (Figure S8). These angular constraints were chosen as both physically reasonable and with a likelihood of matching the measured data for *N* = 10 to *N* = 100 transition dipoles. As expected, the peak *M* values are higher in the FRC than in the FJC model for a given number of transition dipoles. The *M* distributions are shifted to higher values with smaller chain-to-chain angle, as this small angle results in more aligned transition dipoles. For both the 45 and 30 degree angle FRC simulations, the general behavior is the same as that seen in the 3D FJC model, with a shift to higher *M* values and a broadening of the *M* distribution with decreasing *N*.

To best mimic the distribution of polarization modulation values found experimentally for the MEH-PPV molecules prepared from chloroform, a simulated system consisting of *N* = 15 and 8 transition dipoles in ratio of 2:1 with a transition dipole to transition dipole angle of 40 degrees was prepared and then subjected to partial photobleaching. As expected, this led to an increase in median *M* and general shift to higher values in the M distribution and for individual polymers (Figure 5). Figure 5b shows that there was no significant correlation between initial *M* value and intensity change, as expected within this model in which bleaching probability is assigned randomly. In this partial photobleaching simulation, the absolute and relative increases in median M value were less than within the FJC model, suggesting that the relative increase in *M* due to statistical effects depends to some degree on the initial M value and may not be evident in systems in which the *M* distribution is initially centered at a high value.

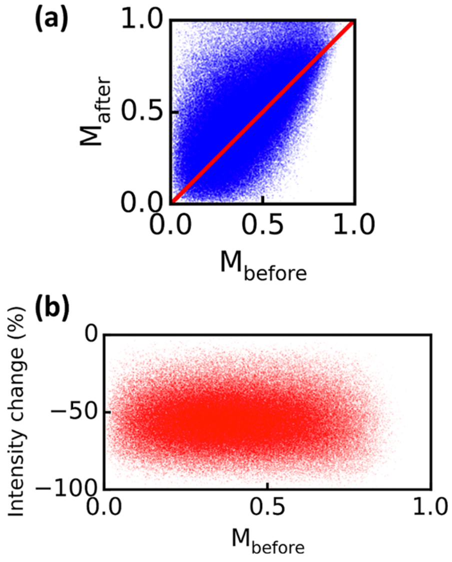

Figure 5. (a) 3D FRC photobleaching simulation for polymers with *N* = 15 and 8 transition dipoles in a ratio of 2:1 and angles between adjacent transition dipoles set to 40°. Bleaching of individual transition dipoles was performed as described in the SI. 100 000 polymers were generated. Median *M* = 0.40 before bleaching and 0.48 after bleaching. (b) Scatter plot of relative intensity change vs initial *M* value for each polymer. Results for pure populations with either *N* = 15 or *N* = 8 transition dipoles are shown in Figure S9.

In the 3D FRC model that most closely matches the experimental data for MEH-PPV molecules dissolved in chloroform in terms of initial *M* distribution, the shift in *M* distribution that occurs due solely to statistical effects is somewhat less than observed in experiment (Figure 2a,c). This suggests that the experimentally observed increases in *M* do not emerge solely from statistical effects. Instead, we suggest that a portion of the observed *M* shift originates from conformation-dependent photostability between and within MEH-PPV polymers. First, examining experimental intensity change with respect to initial *M* value shows that the molecules with the largest relative intensity change are those with low M values initially in both the chloroform and toluene samples (Figure 6). This is distinct from the behavior seen in the simulation (Figure 5b). Experimentally, molecules with low initial *M* values are expected to be present as random coils rather than as highly folded molecules, which would have higher *M* values. In the random coil, efficient across-chain π-orbital interactions are not present, and many isolated chromophores are expected, leading to a correlation between low *M* and high intensity. MEH-PPV with compact, ordered conformations on the other hand have

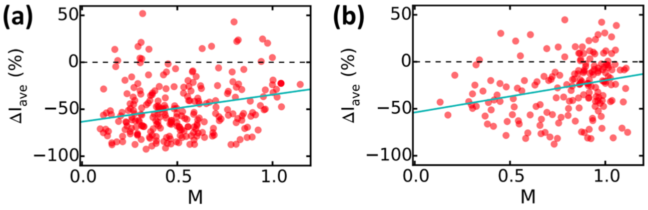

Figure 6. Scatter plots of percentage change of average intensity vs initial *M*. (a) chloroform: median intensity change = −55.1%, fit slope = 28.8, and (b) toluene: median intensity change = −24.1%, fit slope = 34.1.

been shown to have optically dark regions, resulting in correlation between high *M* and relatively dim emission.[33] We confirm this finding by examining average intensity as a function of initial *M* value (Figure 7). The data show that MEH-PPV molecules with higher *M* values (more folded) have less bright emission in both sample systems than those of lower *M* values (more extended).

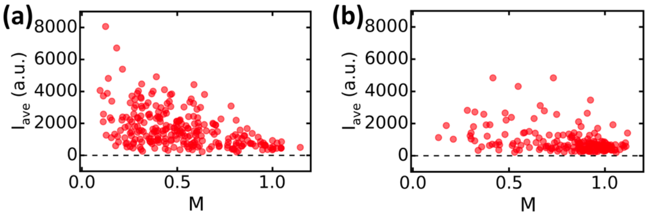

Figure 7. Scatter plots of average intensity vs initial *M*. (a) chloroform: median intensity = 1413 a.u. and (b) toluene: median intensity = 652 a.u.

The experimental observation that molecules with low initial *M* values photobleach more significantly than those with high initial *M* values suggests that molecules with extended conformations are less photostable than those with compact, ordered conformations. This finding within particular samples is also seen across samples, as the relative degree of bleaching of the samples prepared from toluene—composed primarily of molecules with highly ordered conformations—demonstrate significantly less overall intensity decrease during the partial photobleaching than the molecules prepared from chloroform, which have a mixed population of molecular conformations.

Within a given MEH-PPV molecule, evidence for conformation-dependent photobleaching is also evident. In the simulations based on the FRC model, few molecules exhibit a decrease in *M* after partial photobleaching. This can be seen in the average *M* change vs initial *M* (Figure 8a, Figure S9). This behavior differs from experimental results for both chloroform and toluene-prepared MEH-PPV samples. Here, on average, molecules with initially high *M* values display lower *M* values after partial photobleaching. Given that some of these molecules had $M > 1$, we investigated whether this phenomenon could be explained by noise in the *M* measurements but found the result to be insensitive to noise (SI text and Figure S10). These molecules exhibit a change in *M* that opposes that expected from statistical effects, suggesting there is a competing physical process occurring. This competing process is proposed to be conformation-dependent photobleaching within an individual MEH-PPV molecule, with exciton recombination sites present in the folded domains of the polymer bleaching preferentially, leaving behind the chromophores on the more extended regions, an organization of transition dipoles that would drive *M* to lower values. This finding is consistent with the observation and discussion of individual MEH-PPV molecules exhibiting blue-shifted emission over time, a finding that was most obvious in molecules with ordered conformations.[1,2,5,6] It has been proposed that the emitting sites in the ordered domains, to which energy is efficiently funneled, are red-shifted relative to other sites and are relatively photounstable because the excitation spends long times in these sites.

Our findings are summarized schematically in Figure 9. In both molecules, a blue shift upon partial photobleaching is expected as the lower energy sites preferentially photobleach. In the random coil molecule (Figure 9a), these sites are randomly distributed and on average do not affect M. M changes in such molecules then emerge primarily due to statistical effects. The ordered molecule (Figure 9b) exhibits less photobleaching overall relative to those present as random coils. Here, however, the initially bleaching low-lying energy sites are within folded domains, and the preferential bleaching of these sites drives *M* to lower values, overwhelming any change due to statistical effects.

In conclusion, populations of MEH-PPV molecules immobilized in polystyrene typically showed increase in polarization modulation depth upon partial photobleaching. Comparisons to simulations showed a portion of this change was due to statistical effects associated with decreasing number of chromophores. However, experimental measurements showed correlation between the initial *M* value and the degree of photobleaching and between the initial *M* value and the change in *M* value, neither of which was seen in simulation. These experimentally observed correlations suggest that, within a population, molecules with folded conformations are more photostable than those with random coil conformations; however, on a given molecule, domains in folded regions are more susceptible to photobleaching than those outside the collapsed domains, consistent with previous observations of blue-shifted spectra in partially photobleached MEH-PPV

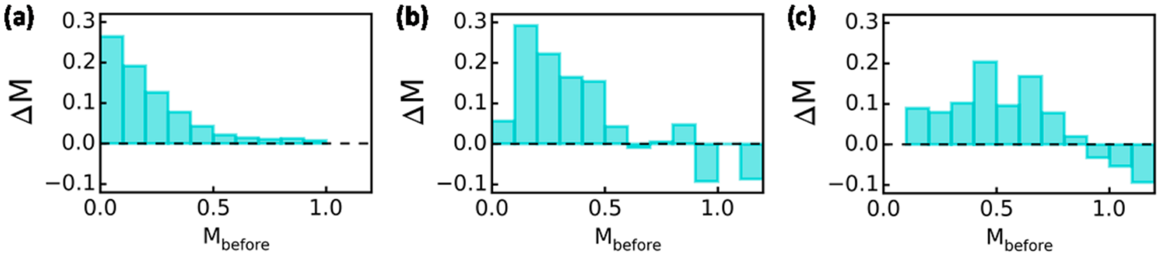

Figure 8. Average *M* change vs initial *M* in (a) the FRC simulation shown in Figure 5, (b) the experiment with MEH-PPV molecules prepared from chloroform, and (c) the experiment with MEH-PPV molecules prepared from toluene.

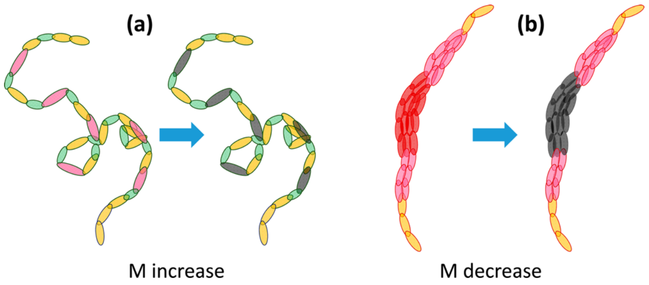

Figure 9. Schematic representation of conformation-dependent photostability and M-change. (a) An extended conformation MEH-PPV molecule with a low M and (b) a folded MEH-PPV molecule with a high M. The red sites are preferentially photobleached, becoming photoinactive (gray).

molecules. This conformational dependence of photobleaching on particular polymers leads to a decrease in M value despite the competing effect from statistics. These findings deepen understanding of the relationship between conjugated polymer molecular conformation and photophysics and in particular the photodegradation that is a critical problem in practical applications of organic materials-based optoelectronic devices. Such understanding may yield insights into enhancing stability and performance of such devices.

ASSOCIATED CONTENT

Supporting Information

The Supporting Information is available free of charge on the ACS Publications website at DOI: 10.1021/acs.nanolett.5b03409.

Materials and methods and supporting figures (PDF)

AUTHOR INFORMATION

Corresponding Author

*E-mail: kaufman@chem.columbia.edu.

Funding

This work was supported in part by the National Science Foundation under CHE 1213242 and a GRF for D.T.H. and in part by the Center for Re-Defining Photovoltaic Efficiency Through Molecule Scale Control, an Energy Frontier Research Center funded by the U.S. Department of Energy, Office of Science, Office of Basic Energy Sciences under DE-SC0001085.

Notes

The authors declare no competing financial interest.

REFERENCES

(1) Huser, T.; Yan, M.; Rothberg, L. J. *Proc. Natl. Acad. Sci. U. S. A.* **2000**, *97*, 11187−11191.

(2) Yu, J.; Hu, D.; Barbara, P. F. *Science* **2000**, *289*, 1327−1330.

(3) Sarzi Sartori, S.; De Feyter, S.; Hofkens, J.; Van der Auweraer, M.; De Schryver, F.; Brunner, K.; Hofstraat, J. W. *Macromolecules* **2003**, *36*, 500−507.

(4) Sun, W. Y.; Yang, S. C.; White, J. D.; Hsu, J. H.; Peng, K. Y.; Chen, S. A.; Fann, W. S. *Macromolecules* **2005**, *38*, 2966−2973.

(5) Liang, J.-J.; White, J.; Chen, Y.; Wang, C.; Hsiang, J.; Lim, T.; Sun, W.; Hsu, J.; Hsu, C.; Hayashi, M.; Fann, W.; Peng, K.; Chen, S. *Phys. Rev. B: Condens. Matter Mater. Phys.* **2006**, *74*, 085209.

(6) Huser, T.; Yan, M. *J. Photochem. Photobiol., A* **2001**, *144*, 43−51.

(7) Lin, H.; Tabaei, S. R.; Thomsson, D.; Mirzov, O.; Larsson, P.-O.; Scheblykin, I. G. *J. Am. Chem. Soc.* **2008**, *130*, 7042−7051.

(8) Adachi, T.; Brazard, J.; Chokshi, P.; Bolinger, J. C.; Ganesan, V.; Barbara, P. F. *J. Phys. Chem. C* **2010**, *114*, 20896−20902.

(9) Furumaki, S.; Habuchi, S.; Vacha, M. *Chem. Phys. Lett.* **2010**, *487*, 312−314.

(10) Lin, H.; Hania, R. P.; Bloem, R.; Mirzov, O.; Thomsson, D.; Scheblykin, I. G. *Phys. Chem. Chem. Phys.* **2010**, *12*, 11770−11777.

(11) Thomsson, D.; Lin, H.; Scheblykin, I. G. *ChemPhysChem* **2010**, *11*, 897−904.

(12) Bounos, G.; Ghosh, S.; Lee, A. K.; Plunkett, K. N.; DuBay, K. H.; Bolinger, J. C.; Zhang, R.; Friesner, R. A.; Nuckolls, C.; Reichman, D. R.; Barbara, P. F. *J. Am. Chem. Soc.* **2011**, *133*, 10155−10160.

(13) Traub, M. C.; Lakhwani, G.; Bolinger, J. C.; Bout, D. V.; Barbara, P. F. *J. Phys. Chem. B* **2011**, *115*, 9941−9947.

(14) Kobayashi, H.; Onda, S.; Furumaki, S.; Habuchi, S.; Vacha, M. *Chem. Phys. Lett.* **2012**, *528*, 1−6.

(15) Mirzov, O.; Bloem, R.; Hania, P. R.; Thomsson, D.; Lin, H.; Scheblykin, I. G. *Small* **2009**, *5*, 1877−1888.

(16) Vogelsang, J.; Brazard, J.; Adachi, T.; Bolinger, J. C.; Barbara, P. F. *Angew. Chem., Int. Ed.* **2011**, *50*, 2257−2261.

(17) Price, G. J.; Smith, P. F. *Polym. Int.* **1991**, *24*, 159−164.

(18) Hu, D.; Yu, J.; Wong, K.; Bagchi, B.; Rossky, P. J.; Barbara, P. F. *Nature* **2000**, *405*, 1030−1033.

(19) Traiphol, R.; Sanguansat, P.; Srikhirin, T.; Kerdcharoen, T.; Osotchan, T. *Macromolecules* **2006**, *39*, 1165−1172.

(20) Ebihara, Y.; Vacha, M. *J. Phys. Chem. B* **2008**, *112*, 12575−12578.

(21) Vacha, M.; Habuchi, S. *NPG Asia Mater.* **2010**, *2*, 134−142.

(22) Tian, Y.; Sheinin, V.; Kulikova, O.; Mamardashvili, N.; Scheblykin, I. G. *Chem. Phys. Lett.* **2014**, *599*, 142−145.

(23) Park, H.; Hoang, D. T.; Paeng, K.; Kaufman, L. J. *ACS Nano* **2015**, *9*, 3151−3158.

(24) Neef, C. J.; Ferraris, J. P. *Macromolecules* **2000**, *33*, 2311−2314.

(25) An open source Python project: https://github.com/soft-matter/trackpy, 2015.

(26) Crocker, J. C.; Grier, D. G. *J. Colloid Interface Sci.* **1996**, *179*, 298−310.

(27) Moscatelli, A.; Livingston, K.; So, W. Y.; Lee, S. J.; Scherf, U.; Wildeman, J.; Peteanu, L. A. *J. Phys. Chem. B* **2010**, *114*, 14430−14439.

(28) DuBay, K. H.; Hall, M. L.; Hughes, T. F.; Wu, C.; Reichman, D. R.; Friesner, R. A. *J. Chem. Theory Comput.* **2012**, *8*, 4556−4569.

(29) Köhler, A.; Hoffmann, S. T.; Bässler, H. *J. Am. Chem. Soc.* **2012**, *134*, 11594−11601.

(30) Tian, Y.; Kuzimenkova, M. V.; Halle, J.; Wojdyr, M.; Diaz de Zerio Mendaza, A.; Larsson, P.-O.; Müller, C.; Scheblykin, I. G. *J. Phys. Chem. Lett.* **2015**, *6*, 923−927.

(31) Mirzov, O.; Scheblykin, I. G. *Phys. Chem. Chem. Phys.* **2006**, *8*, 5569−5576.

(32) Teraoka, I. *Polymer solutions: An introduction to physical properties*; Wiley: New York, 2002; p 338.

(33) Lin, H.; Tian, Y.; Zapadka, K.; Persson, G.; Thomsson, D.; Mirzov, O.; Larsson, P.-O.; Widengren, J.; Scheblykin, I. G. *Nano Lett.* **2009**, *9*, 4456−4461.